Journal of
Marine Science and Engineering

MDPI

Article

Multi-Objective Production and Scheduling Optimization of Offshore Wind Turbine Steel Pipe Piles Based on Improved Hesitant Fuzzy Method

Weihan Wang [1,2,3], Jinchao Xiao [2,3,*], Dongying Feng [2], Sanxi Wei [2] and Zhongze Wang [2,3,4]

[1] College of Chemical Process Automation, Shenyang University of Technology, Shenyang 110870, China
[2] Guangzhou Institute of Industrial Intelligence, Guangzhou 511458, China
[3] Shenyang Institute of Automation, Chinese Academy of Sciences, Shenyang 110016, China
[4] University of Chinese Academy of Sciences, Beijing 100049, China
* Correspondence: xiaojinchao@sia.cn

Abstract: This paper investigates the multi-objective optimization problem in the production of offshore wind turbine steel pipe piles (OWTSPP). Considering the particularity of the steel pipe pile production process, it is divided into a flexible flow shop scheduling (FFSS) stage and an open parallel shop scheduling (OPSS) stage, respectively. Mathematical models are established for each stage, and the critical path and production time information are obtained using a disjunctive graph model. Due to the inability of existing empirical scheduling methods to balance production goals, an improved Pythagorean hesitant fuzzy method (IPHFM) is proposed to solve the multi-objective optimization problem in steel pipe pile production. Specifically, the maximum completion time, machine total load, and total completion time are taken as optimization objectives. The improved Lagrange multiplier method with penalty terms is used to handle the constraints and objective functions, and a Lagrange objective function is generated. Then, the Lagrange objective function matrix is obtained by normalization and same-scale processing, and an algorithm is designed to obtain the Pareto front solution set. Finally, this paper compares the optimal scheduling plans under the empirical scheduling method and the improved method. The results show that the improved method can significantly improve production efficiency in both small-scale and large-scale production, with improvements of 15.7% and 22.16%, respectively.

Keywords: offshore wind turbine steel pipe piles (OWTSPP); flexible flow shop scheduling (FFSS); open parallel shop scheduling (OPSS); disjunctive graph model; multi-objective optimization; improved Pythagorean hesitant fuzzy method (IPHFM)

check for updates

Citation: Wang, W.; Xiao, J.; Feng, D.; Wei, S.; Wang, Z. Multi-Objective Production and Scheduling Optimization of Offshore Wind Turbine Steel Pipe Piles Based on Improved Hesitant Fuzzy Method. *J. Mar. Sci. Eng.* **2023**, *11*, 1505. https://doi.org/10.3390/jmse11081505

Academic Editor: Pedro Jesús Cabrera Santana

Received: 30 June 2023
Revised: 22 July 2023
Accepted: 26 July 2023
Published: 28 July 2023

1. Introduction

With the vigorous development of renewable energy, it is crucial to improve the production efficiency of Offshore Wind Turbine Steel Pipe Piles (OWTSPP), which are widely used as the foundation in offshore wind farms. As one of the largest wind power markets globally, China recognizes the significance of efficient and high-quality OWTSPP production as a key manifestation of industrial competitiveness. Therefore, enhancing the production efficiency and quality of OWTSPP holds great importance in promoting the development of the renewable energy industry and strengthening enterprise competitiveness.

Considering the current situation where enterprises rely on experience scheduling, the production efficiency is low, and the production of various types of OWTSPP may be disorderly when urgent production occurs. Figure 1 shows the key steps involved in the OWTSPP production process, including cutting, splicing, rolling, longitudinal welding, and circumferential welding. Among them, the cutting, splicing, and rolling processes can be regarded as FFSS, while the longitudinal and circumferential welding can be seen as OPSS.

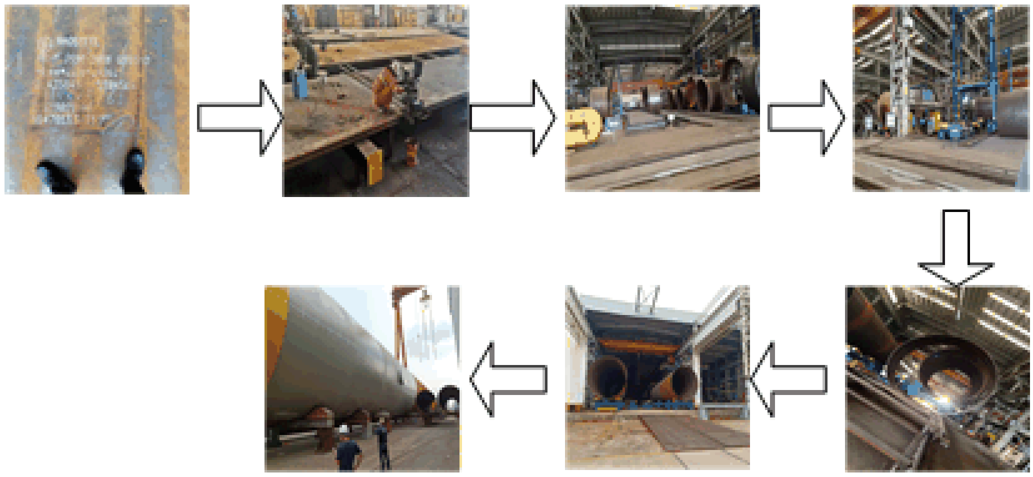

Figure 1. The Production Process of OWTSPP.

The research on scheduling problems can be traced back to the mid-1950s [1]. With the rapid development of artificial intelligence technology, intelligent manufacturing has become increasingly popular, which undoubtedly promotes the research of optimization scheduling algorithms, multi-objective optimization, and other aspects. Both FFSS and OPSS problems are very valuable for research, and multi-objective optimization has been a research hotspot in recent years [2–7]. In recent years, researchers have used various algorithms, improved algorithms, and reinforcement learning methods to solve various workshop scheduling problems [8–13], as well as various multi-objective optimization scheduling problems [14–19]. At the same time, research methods are relatively mature, including optimization theory research, algorithm improvement simulation research methods to improve optimization capabilities and achieve better convergence results [20,21]. In addition, researchers have combined improved methods with real production data to conduct multi-objective optimization studies in workshop production, which is also a very important research method [22].

It should be emphasized that all scheduling optimization methods must be combined with actual production. In production, it is necessary to consider how to optimize multiple objectives such as project duration, machine utilization, and total production time in an uncertain environment [23–25]. Since fuzzy methods can solve uncertainty problems well, more and more scholars have started to study scheduling problems under various uncertain environments, including uncertain delivery dates, uncertain scheduling start and end times [26–32]. In terms of multi-objective optimization, fuzzy methods have also been widely used, such as multi-objective optimization priori weighting, multi-stage multi-objective optimization, and constrained multi-objective optimization examples [33–38].

With the emergence of Pythagorean fuzzy methods, fuzzy methods have become more flexible in making actual problem decisions and optimizations [39,40]. Zhang expanded the use of interval representation for membership, non-membership, and hesitation information based on Pythagorean fuzzy method [41]. Liu Weifeng et al. combined the advantages of Pythagorean fuzzy method and hesitant fuzzy method and used the expert scoring simulation and assigning decision influencing factor weights to obtain the multi-objective ranking results under multiple criteria [42,43]. When considering the weight of unknown decision objectives, it is impossible to obtain a score function or determine the optimal solution ranking. In this case, the multi-objective decision-making problem can be viewed as a multi-objective optimization problem. Finally, an improved Pythagorean hesitant fuzzy method was used to discuss and study the multi-objective optimization problem.

2. Description of Production Problems for OWTSPP

OWTSPP can be regarded as workpieces with multiple processes, and each process has multiple processing machines to choose from. Due to the particularity of the production process of OWTSPP, the process is decomposed into FFSS and OPSS, and solutions are obtained based on these two scheduling problems.

According to the production situation of OWTSPP in the enterprise, the symbols used in the process of establishing mathematical models are explained as shown in Part (a) of Nomenclature Section.

Based on production data from the enterprise, a disjunctive graph model is used to provide slack time for non-production processes and to identify the critical path in order to ensure scheduling accuracy. In Figure 2, M_1, M_2 and M_3 represent different types of processing machines and are depicted in different colors. The workflow is represented by the start and end nodes $Start - End$ while O_{ij} denotes the jth operation of workpiece i. Directed line segments are used to represent the time required to transition from one production stage to another, including non-production time.

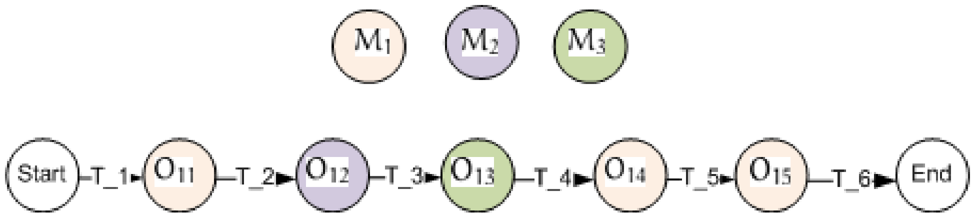

Figure 2. The Disjunctive Graph Model for a Certain Type of OWTSPP.

2.1. Mathematical Model for Flexible Flow Shop Scheduling Stage

In the production of OWTSPP, the steel plate splicing, cutting, and rolling processes form a serial machine environment, with a, b, and c parallel machines for each stage respectively. Let M be the set of all machines, m be the number of production machines for OWTSPP, and n be the number of steel plates produced. Moreover, workpieces can be stored indefinitely between any two consecutive stages. Therefore, the steel plate splicing, cutting, and rolling processes conform to the characteristics of FFSS and can be regarded as a FFSS model (as shown in Figure 3).

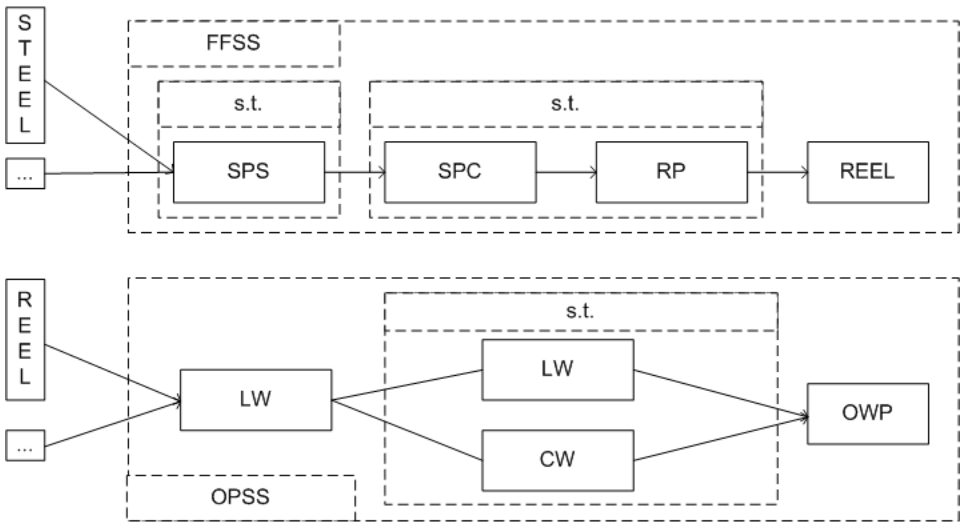

Figure 3. Breakdown Chart of OWTSPP Production Process.

In the FFSS stage of OWTSPP production, a mathematical model for FFSS is established based on the mathematical symbols listed in Part (a) "Mathematical Symbols and Interpretation" of Nomenclature Section. The objective function is formulated according to actual production situations, and constraint conditions are also specified.

The objective functions considered in this paper are total completion time, maximum completion time, and machine utilization rate. They are formulated according to actual production situations as follows:

(1) Minimizing maximum completion time.

$$f_1 = min(max_{j \in J} max_{o \in O}(c_{j,o,m}))$$

(2) Minimizing machine total load.

$$f_2 = min(\sum_{m=1}^{m} \sum_{o \in O} \sum_{j=1}^{n} (t_{j,o,m} \cdot x_{j,o,m}))$$

(3) Minimizing total completion time.

$$f_3 = \min(\sum_{j=1}^{n} \sum_{m=1}^{m} (t_j^x + t_j^y + t_j^z) x_{j,o,m})$$

The constraint conditions are specified according to the production process in the FFSS stage.

$$\text{s.t.} \begin{cases} \sum_{j=1}^{n} x_{j,o,m} = 1, & \forall o \in O, \forall m \in M \\ \sum_{m=1}^{m} x_{j,o,m} = 1, & \forall j \in J, \forall o \in O \\ s_{j,o,m} + t_{j,o,m} \le s_{j,o+1,m}, & \forall j \in J, \forall o+1 \in O, \forall m \in M \\ c_{j,o,m} \le c_{j+1,o,m}, & \forall j+1 \in J, \forall o \in O, \forall m \in M \\ c_{j,o,m} \le s_{j,o+1,m}, & \forall j \in J, \forall o+1 \in O, \forall m \in M \\ s_{j,o,m} = 0, & \forall j \in J \\ s_{j,o,m} + t_{j,o,m} \le s_{j,o+1,m}, & \forall j \in J, \forall o \in O, \forall m \in M \\ t_{j,o,m} \ne t_{j',o,m}, & \forall j \ne j', \forall j, j' \in J, \forall o \in O, \forall m \in M \\ \sum_{m=1}^{M} x_{j,o,m} \ge 2, & \forall j \in J, \forall o \in O \\ x_{j,o,m} = x_{j,o,m'}, & \forall j \in J, \forall o \in O, \forall m, m' \in M \end{cases}$$

(1) One machine can only process one operation of a steel pipe pile at a certain point in time; (2) Only one machine can process the same operation of the same steel pipe pile at the same time; (3) Once the processing of an operation for a steel pipe pile starts, it cannot be interrupted; (4) The processing priority is the same for different OWTSPP; (5) The processing of operations among different OWTSPP has no order constraints, but the operations of the same steel pipe pile have precedence constraints. (6) The first operation of any steel pipe pile can be processed at time zero; (7) Each steel pipe pile must be processed in the order of steel plate splicing, cutting, and rolling; (8) The operations are the same for different OWTSPP, but their processing times are different; (9) Each steel pipe pile must be processed in the order of steel plate splicing, cutting, and rolling; (10) The same machine is used for the same operation of any steel pipe pile.

2.2. Mathematical Model for Open Parallel Shop Scheduling Stage

Both circumferential seam welding and longitudinal seam welding use the same welding machine for production. Under the condition of meeting the constraint conditions, these two production processes can be viewed as an OPSS model, see Figure 3.

To accurately define the OPSS model, the following names are given to the reels at different welding stages: (1) Unwelded reel refers to the reel that has not undergone longitudinal seam welding; (2) Longitudinally welded reel refers to the reel that has undergone longitudinal seam welding but not circumferential seam welding; (3) Reel refers to all reels that do not need to be specified for a particular stage. To facilitate understanding, the mathematical symbol explanations are added as follows:

n: The quantity of reels that have completed longitudinal seam welding.
m: The number of welding machines.
A_j: The remaining quantity of reels that have completed longitudinal seam welding, i.e., the quantity of reels that can undergo circumferential seam welding.
P_j: The number of circumferential seam welding operations.

The objective function for OPSS is as follows:
(1) Minimizing total completion time.

$$f_5 = \min(\sum_{j=1}^{n}\sum_{m=1}^{m}(t_j^p + t_j^a)x_{j,o,m})$$

(2) Minimizing machine total load.

$$f_2 = min(\sum_{m=1}^{m}\sum_{o\in O}\sum_{j=1}^{n}(t_{j,o,m} \cdot x_{j,o,m}))$$

(3) Minimizing maximum completion time.

$$f_1 = min(max_{j\in J} max_{o\in O}(c_{j,o,m}))$$

The constraint conditions are specified based on the characteristics of OPSS and the production situation of longitudinal seam welding and circumferential seam welding as follows:

$$\text{s.t.} \begin{cases} \sum_{j=1}^{n} x_{j,o,m} \leq 1, & \forall m \in M \\ A_j \geq 2P_j, & \forall j \in J \\ A_j = A_{j'} - 2n, & \forall m \in M, j, j' \in J, j' \neq j \\ A_j = A_{j'} + n, & \forall m \in M, j, j' \in J, j' \neq j \\ \sum_{j=1}^{n} x_{j.o.m} \leq 1, & \forall m \in M \\ t_j^a \leq t_j^p, & \forall j \in J \\ m < n & \\ A_j \geq P_j, & \forall j \in J \end{cases}$$

(1) Each welding machine can only participate in the welding of one reel at a time; (2) Circumferential welding can only be carried out when there are at least 2 surplus reels ($A_j \geq 2$) after longitudinal seam welding has been completed. Here, P_j represents the number of circumferential welds; (3) After each circumferential welding operation, the number of reels that have completed longitudinal seam welding will be reduced by 2 (j' represents the ID of another reel different from j); (4) After each longitudinal seam welding operation, the number of reels that have completed longitudinal seam welding will be increased by 1; (5) The welding machines can be reused in cycles, and any reel at any stage can be welded by a free welding machine; (6) The time required for longitudinal seam welding is different from the time required for circumferential seam welding, and the time required for longitudinal seam welding is less than that for circumferential seam welding; (7) There are welding machines available, and there are a large number of reels to be welded, far more than the number of welding machines available; (8) Longitudinal seam welding and circumferential seam welding are different processes in the production of the workpiece, and circumferential seam welding can only be carried out after longitudinal seam welding.

3. Analysis and Processing of Production Data for OWTSPP

To facilitate reading of this chapter, the abbreviated names and meanings of production processes and unit symbols are listed in Part (b) of Nomenclature Section. The production process of OPW is shown in the schematic diagram below (refer to Figure 4), which can be aided by Part (b) of Nomenclature Section for better understanding.

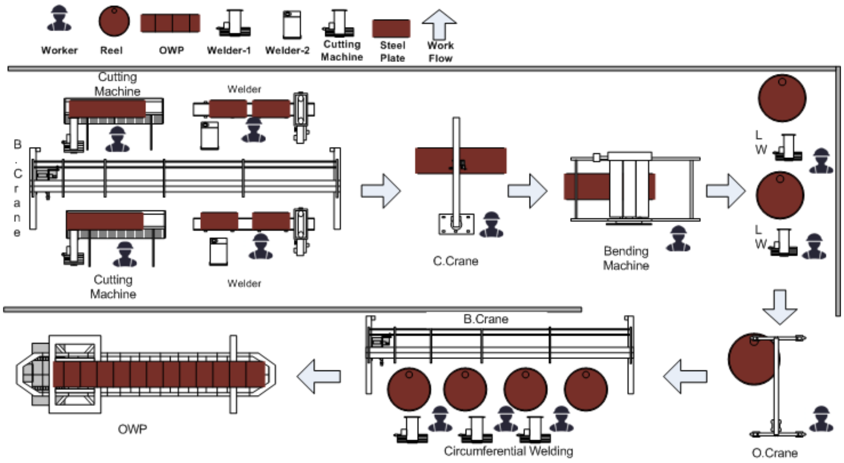

Figure 4. Diagram of Key Production Processes for OWTSPP.

The enterprise has provided production data for a certain type of OWTSPP. Table 1 has processed the production data. It should be pointed out that the internal and external group welding method is often used in the longitudinal and circumferential seam welding stages.

Table 1. Production Information Table for a Certain Type of OWTSPP.

ShortHand	SPS	SPC	RP	LW	CW
W.H (h/day)	20	22	20	20	20
WCM-1 (kg/m)	15	-	-	15	15
WCM-2 (kg/h)	7.5	-	-	7.5	7.5
MPC (m)	810	607.5	675	675	810
Workstation (WS)	5	2	2	3	4
WH	5.4	2.7	2	5.4	8.4
SW Pro.E (mm/min)	-	200	120	-	-
OWTSPPPF	34	34	34	34	17
SW Prod. E (m/h/WS)	0.5	12	132	0.5	0.5

Analyzing the data in Table 1 provides detailed production information for the OWTSPP. Due to space limitations, this article does not elaborate on the detailed production information of other types of OWTSPP. Only key information such as workpiece J, machine M, process O, and time t_j^x, t_j^y, t_j^z, t_j^a, t_j^b are given. To simplify the problem difficulty, the steel pipe pile is treated as one workpiece.

3.1. Processing of OWTSPP Production Data

This chapter records the processing time in hours for five different types of OWTSPP on different machines (see Table 2). These data provide a basis for further optimizing the production process.

Table 2. Schedule for OWTSPP Processing.

Process / Type	SPS	SPC	RP	LW	CW
OWTSPP-1	5.4	2.7	2	5.4	16.8
OWTSPP-2	4.3	2.2	1.8	4.3	12.4
OWTSPP-3	8.1	4.2	2.5	8.1	17.6
OWTSPP-4	9	4.7	2.4	9	22.4
OWTSPP-5	6.2	2.9	2.2	6.2	18.6

Based on the production time data of different processes for different types of OWTSPP in Table 2, a disjunctive graph model is established (see Figure 5). In this model, the influence of slack time is not considered, and each workpiece is regarded as a path. A directed acyclic graph is used to represent the order of different steel pipe pile processes.

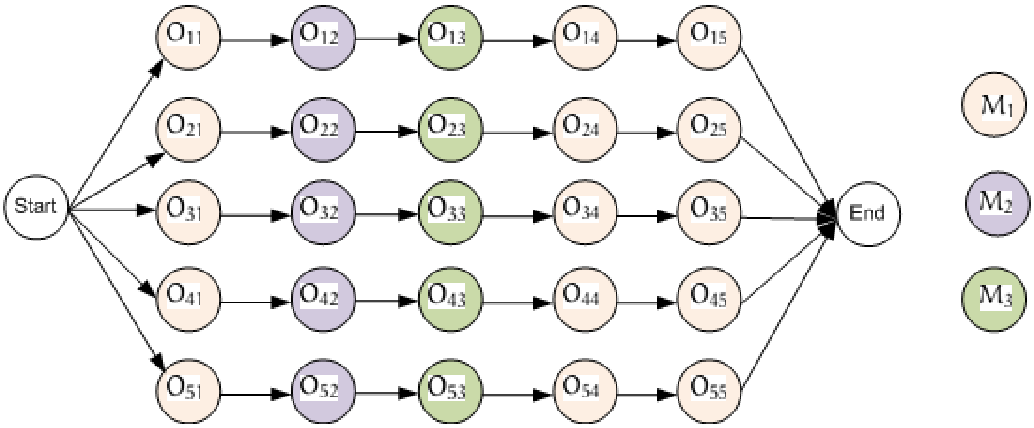

Figure 5. Disjunctive Graph Models for Different Types of OWTSPP.

In the Figure 5, $O_{11}, O_{12}, O_{13}, O_{14}, O_{15}$ represent the five processes involved in OWTSPP production, namely splicing, cutting, coiling, longitudinal seam welding, and circumferential peak welding.

3.2. Flexible Flow Shop Scheduling Stage Data Processing

It is known that this stage includes three steps: O_{11}, O_{12}, O_{13}, as shown in Figures 6 and 7. The reel can be regarded as a finished workpiece j, so the processing time of workpiece$j$ on the three steps in the FFSS is $t_j = t_a + t_b + t_c$. Table 3 records the number of processing machines and corresponding processing times required for five different types of OWTSPP in the first three processes.

Table 3. FFSS Stage Production Time Information Table.

Job	Operation	$m_{1–5,10–12}$	$m_{6–7}$	m_8	m_9
	o_{11}	5.4	-	-	-
j_1	o_{12}	-	2.7	-	-
	o_{13}	-	-	2	3
	o_{11}	4.3	-	-	-
j_2	o_{12}	-	2.2	-	-
	o_{13}	-	-	1.8	2.7
	o_{11}	8.1	-	-	-
j_3	o_{12}	-	4.2	-	-
	o_{13}	-	-	2.5	3.8
	o_{11}	9	-	-	-
j_4	o_{12}	-	4.7	-	-
	o_{13}	-	-	2.4	3.6
	o_{11}	6.2	-	-	-
j_5	o_{12}	-	2.9	-	-
	o_{13}	-	-	2.2	3.3

Figure 6 represents the distribution of processing times on different machines. It showcases the processing times of these five types of OWTSPP in different processes using a 3D surface plot and a 3D scatter plot.

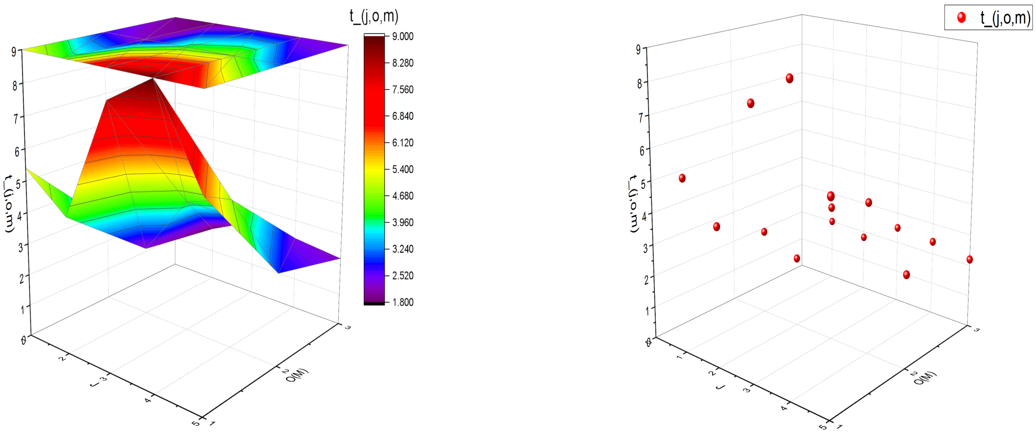

3D colormap surface Image 3D scatter Image

Figure 6. Machine Distribution Image for Different Workpiece Processes in the FFSS Stage.

Assign the processing time of the first three stages to the diagram in Figure 5, and we get the disjunctive graph with the processing time of the first three stages. Figure 7 clearly represents the production time for each production process.

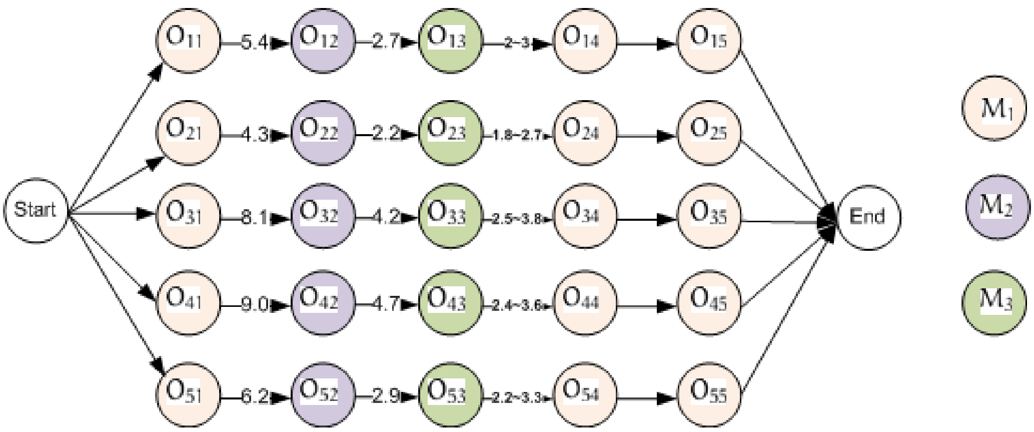

Figure 7. FFSS Stage Disjunctive Graph Model.

3.3. Open Parallel Shop Scheduling Data Processing

According to Figures 8 and 9, this stage includes two production processes, O_{14},O_{15}, with the recording of the production time for the last two processes. Table 4 records the processing time for different types of OWTSPP on different machines during longitudinal seam welding and circular seam welding processes.

Table 4. OPSS Stage Production Time Information Table.

Job	Operation	$m_{1\text{–}5,10\text{–}12}$	$m_{1\text{–}5,10\text{–}12}$
j_1	o_{14}	5.4	-
	o_{15}	-	16.8
j_2	o_{24}	4.3	-
	o_{25}	-	12.4
j_3	o_{34}	8.1	-
	o_{35}	-	17.6
j_4	o_{44}	9	-
	o_{45}	-	22.4
j_5	o_{54}	6.2	-
	o_{55}	-	18.6

Figure 8 illustrates the distribution of different types of steel pipe pile processes, machines, and production times during the OPSS stage.

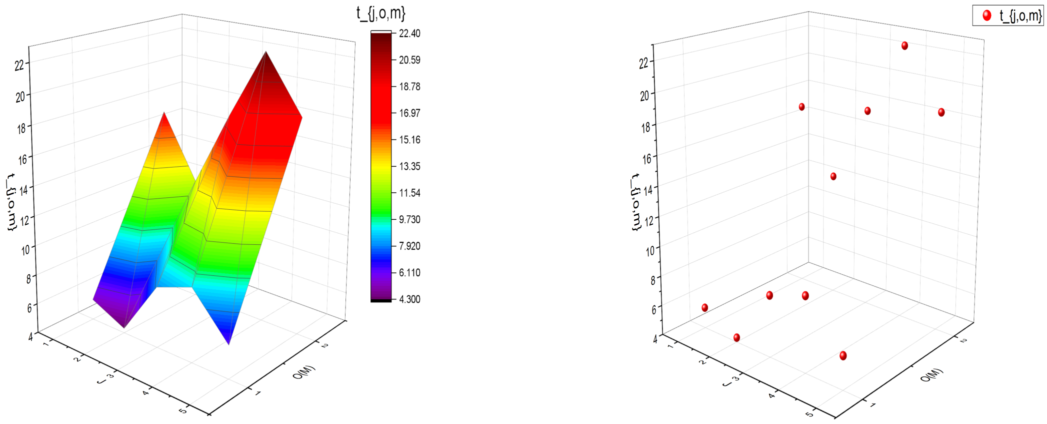

3D Colormap Surface Image 3D Scatter Image

Figure 8. Machine Distribution Image for Different Workpiece Processes in the OPSS Stage.

By adding the processing time of the last two processes in the OPSS stage to Figure 5, we obtain the disjunctive graph model shown in Figure 9. The figure clearly illustrates the production process of OWTSPP and the production time for processes 4 and 5 of different types of OWTSPP.

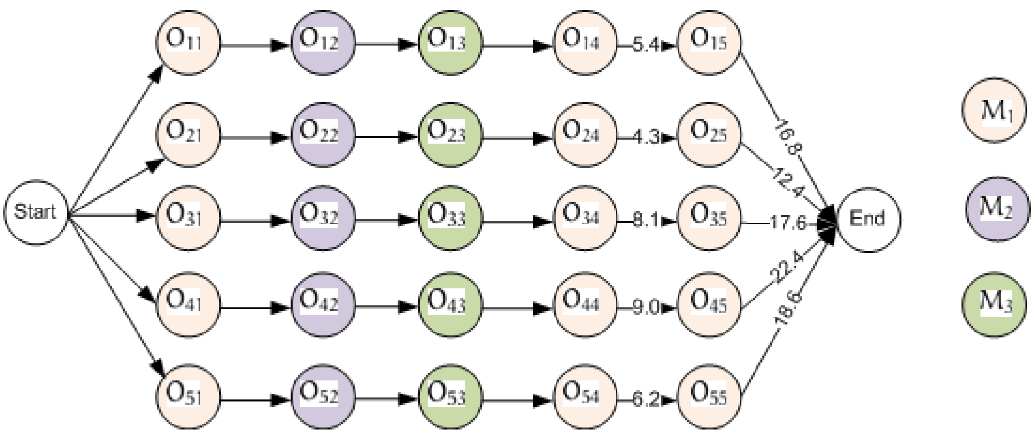

Figure 9. OPSS Disjunctive Graph Model.

3.4. Slack Time Analysis

During the production process, uncertainties such as machine efficiency, labor efficiency, and transfer time in each production process can lead to situations of early completion or delays. Therefore, based on the production times provided in Tables 3 and 4, it is necessary to consider production slack time t_{si}. In order to cope with possible production delays, a certain slack time is allocated for each production process. The processed ranges of slack time for different types of OWTSPP and different production processes are presented in Table 5.

Table 5. Slack Time Table.

Type \ Process	Step-1	Step-2	Step-3	Step-4	Step-5
OWTSPP-1	0.2–0.4 h	0.4–0.8 h	0.4–0.6 h	0.4–0.8 h	0.4–0.8 h
OWTSPP-2	0.2–0.4 h	0.4–0.8 h	0.4–0.6 h	0.4–0.8 h	0.4–0.8 h
OWTSPP-3	0.2–0.4 h	0.4–0.8 h	0.4–0.6 h	0.4–0.8 h	0.4–0.8 h
OWTSPP-4	0.2–0.4 h	0.4–0.8 h	0.4–0.6 h	0.4–0.8 h	0.4–0.8 h
OWTSPP-5	0.2–0.4 h	0.4–0.8 h	0.4–0.6 h	0.4–0.8 h	0.4–0.8 h

The Table 5 includes information about the slack time for each production stage. When considering slack time, the total production time for the entire process is t_j, in which case the critical path is $C = t_j$.

$$t_j = t_j^x + 4t_{s1} + t_j^y + 4t_{s2} + t_j^z + 2t_{s3} + t_j^a + 2t_{s4} + t_j^b + t_{s5}$$

To ensure the uncertain characteristics of slack time, for each circumferential seam welding, 4 cutting operations, 8 splicing operations, 2 rolling operations, and 2 longitudinal seam weldings are required. After adding the production slack time to the production time of each process, all possible production times for this process are obtained. The sum of the production times for all processes is the total production time of the OWTSPP, which results in the disjunctive graph model for the entire production process with slack time, as shown in Figure 10.

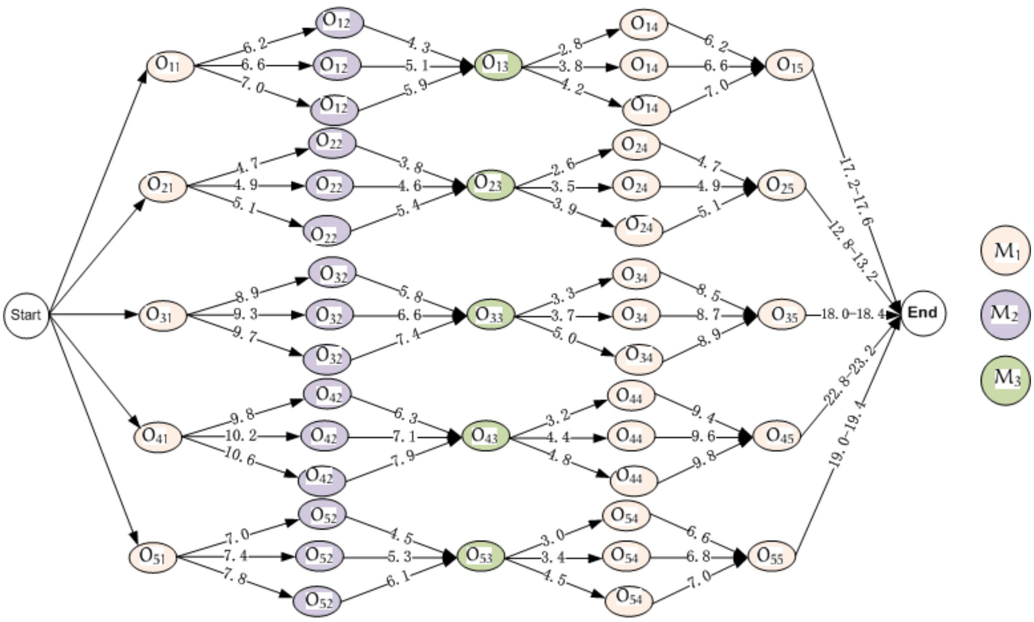

Figure 10. Disjunctive Graph Model for Production Process with Possible Production Time.

The figure includes the possible production times for each stage, dividing all possible production times into three groups, as indicated by the time shown in each of the three paths in the figure. From Figure 10, it can be seen that the numbers on the directed line segments represent the production times of the processes considering the slack time. The critical path is the longest path in terms of time duration in the production process and represents the minimum time required to complete the production, and the critical path C considering slack time is as follows: $C = 10.6 + 7.9 + 4.8 + 9.8 + 23.2 = 56.3$.

4. Research on Improving Pythagorean Hesitant Fuzzy Method

The Pythagorean hesitant fuzzy method usually uses a ternary array $A = \{< x, \Gamma_A(x), \Psi_A(x) > | x \in X\}$ to represent the attribute information of decision alternatives, where $\Gamma_A(x)$ and $\Psi_A(x)$ are non-empty finite subsets belonging to [0, 1]. It also satisfies $\mu_A^2(x) + \nu_A^2(x) \leq 1$, where $\forall x \in X$ and $\forall \mu_A(x) \in \Gamma_A(x)$,$\forall \nu_A(x) \in \Psi_A(x)$correspond to the weights of different attributes under different decision alternatives. According to the decision matrix, the score function of each alternative is calculated, and finally, the alternatives are ranked according to the size of their score functions for selection and optimization [42,44].

This article uses a multivariate array $< t, t', x, f_1, f_2, f_3, g_n, g_m >$ to replace the ternary array under hesitant fuzzy sets. Among them, t, t' and x are the parameters involved in the target function optimization process, while f_1,f_2, and f_3 represent the objective functions that need to be optimized. At the same time, considering multiple constraints $g_i(x)$, when conducting multi-objective optimization, weight factors are ignored, and the Lagrange multiplier method with penalty terms is used to handle different objective functions and constraints, which is transformed into the Lagrange objective function $L_i(t, t', x, \lambda, \varepsilon)$. Finally, the Lagrange objective function matrix X, is solved, and the Pareto front solution set is found according to Algorithm 1 and 2.

Algorithm 1 Pareto Front Algorithm with Simulated Annealing

Input:
- X: Objective function vector matrix
- T_0: Initial temperature
- T_{end}: Termination temperature
- α: Cooling rate

Output:
- PF: Pareto front set

PF = Pareto-Front-Algorithm(X)

while $T_0 > T_{end}$ **do**
    $Q = \emptyset$
    for each x in PF **do**
        y = SA(x, T_0) // apply SA for vector optimization
        add-to-Q(y, Q) // add optimized solution to Pareto front
    end for
    PF = merge (PF, Q)
    $T_0 = \alpha * T_0$ // cooling down
end while
return PF

Algorithm 1 serves as the main framework for filtering Pareto front solutions, including the starting and stopping conditions, optimization process, and secondary screening of optimal solutions. Algorithm 2, on the other hand, represents the classical Pareto front algorithm, primarily comparing the distance between objective function vectors to determine non-dominated solutions and conducting a primary screening of Pareto front solutions.

4.1. Processing of Constraint Conditions in the Production Stage of OWTSPP

When processing the constraint conditions in the scheduling stage of a FFSS, the constraint conditions are added to the objective function, and the augmented Lagrangian multiplier method is used to convert multiple equality and inequality constraints into unconstrained optimization problems [45–47]. By introducing the Lagrangian multiplier vector $\lambda = (\lambda_1, \ldots, \lambda_m)^\top$ and penalty term ε, the constraint conditions are transformed into equality constraints [48,49]. Multiple constraint conditions are represented as $L(x, \lambda) = f(x) + \lambda^\top g(x)$ after being processed by the Lagrangian multiplier. Here

$f : R^n \rightarrow R^1$, $g : R^n \rightarrow R^m$, $g(x) = [g_1(x), g_2(x), \ldots, g_m(x)]^\top$, and $\varepsilon > 0$ is the penalty term. The augmented Lagrange objective function with penalty terms is defined as follows:

Algorithm 2 Pareto-Front-Algorithm

```
Input:
        - d: Euclidean distance
        - ω: Distance weight factor
        -X: Objective function matrix
Output:
        - PF: Pareto front set
PF =()

for i = 1 to N do
    p = the i-th solution
    flag = True
    for j = 1 to |PF| do
        q = the j-th solution in the PF
        d = sqrt((X_ij(t, t', x) − X_i'j'(t, t', x))^2)
        if d <= ω * w(j) then
            flag = False
            break
        end if
    end for
end for
return PF
```

$$L(t_{j,o,m}, c_{j,o,m}, s_{j,o,m}, x_{j,o,m}, \lambda, \varepsilon) = f(x) + \lambda^\top g(x) + \varepsilon||g(x)||^2$$

Here, x represents the variables in the constraint conditions and objective function during production, which are not further elaborated. For ease of reading, $s_{j,o,m}$ and $c_{j,o,m}$, which represent the start and end times of processing, are denoted as t', while t_j^x, t_j^y, t_j^z and $t_{j,o,m}$, which represent the processing time, are denoted as t, and substituted into the formula.

The constraint conditions are processed as follows:

$$\text{s.t.} \begin{cases} g_1(x) = \sum_{j=1}^{n} x_{j,o,m} - 1 = 0 & \forall o \in O, \forall m \in M \\ g_2(x) = \sum_{m=1}^{m} x_{j,o,m} - 1 = 0 & \forall j \in J, \forall o \in O \\ g_3(s,t) = s_{j,o,m} + t_{j,o,m} - s_{j,o+1,m} \leq 0 & \forall j \in J, \forall o+1 \in O, \forall m \in M \\ g_4(c) = c_{j,o,m} - c_{j+1,o,m} \leq 0 & \forall o \in O, \forall m \in M \\ g_5(c,s) = c_{j,o,m} - s_{j,o+1,m} \leq 0 & \forall j \in J, \forall o+1 \in O, \forall m \in M \\ g_6(s) = s_{j,o,m} = 0 & \forall j \in J \\ g_7(s,t) = s_{j,o,m} + t_{j,o,m} - s_{j,o+1,m} \leq 0 & \forall j \in J, \forall o \in O, \forall m \in M \\ g_8(t) = t_{j,o,m} - t_{j',o,m} \neq 0 & \forall j \neq j', \forall j, j' \in J, \forall o \in O, \forall m \in M \\ g_9(x) = \sum_{m=1}^{M} x_{j,o,m} - 2 \geq 0 & \forall j \in J, \forall o \in O \\ g_{10}(x) = x_{j,o,m} - x_{j,o,m'} = 0 & \forall j \in J, \forall o \in O, \forall m, m' \in M \end{cases}$$

In the FFSS problem, the augmented Lagrangian multiplier method is used to combine the 10 constraints and the objective function into an unconstrained optimization problem. The Lagrangian function can be obtained by combining the objective function (1) with corresponding constraint conditions (1)–(10) as follows:

$$\underset{t'}{L}(t', \sum_{i=1}^{10} \lambda_i, \sum_{i=1}^{10} \varepsilon_i) = f_1(t') + \sum_{i=1}^{10} \sum_{i=1}^{10} \lambda_i g_i(t') + \sum_{i=1}^{10} \sum_{i=1}^{10} \varepsilon_i ||g_i(t')||^2$$

Similarly, the Lagrangian objective function formed by combining the objective functions (2) and (3) with constraints (1)–(10) is as follows:

The processed result of the objective function (2) is as follows:

$$\underset{t,x}{L}(t,x,\sum_{i=1}^{10}\lambda_i,\sum_{i=1}^{10}\varepsilon_i)=f_2(t,x)+\sum_{i=1}^{10}\sum_{i=1}^{10}\lambda_i g_i(t,x)+\sum_{i=1}^{10}\sum_{i=1}^{10}\varepsilon_i||g_i(t,x)||^2$$

The processed result of the objective function (3) is as follows:

$$\underset{t,x}{L}(t,x,\sum_{i=1}^{10}\lambda_i,\sum_{i=1}^{10}\varepsilon_i)=f_3(t,x)+\sum_{i=1}^{10}\sum_{i=1}^{10}\lambda_i g_i(t,x)+\sum_{i=1}^{10}\sum_{i=1}^{10}\varepsilon_i||g_i(t,x)||^2$$

The objective function above shows the constraints treated with penalty terms using the Lagrange multiplier method, and the objective function, objective function vector, processed constraints, and other information are unified into the improved fuzzy method for subsequent normalization and scaling of the objective function in the FFSS Stage.

Similarly, the constraint conditions for the OPSS problem are organized and unified into functional forms of equations or inequalities for ease of handling. The summarized constraint conditions are as follows:

$$\text{s.t.}\begin{cases} k_1(x)=\sum\limits_{j=1}^{n}x_{j,o,m}-1\le 0 & \forall m\in M\\ k_2(A,P)=A_j-2P_j\ge 0 & \forall j\in J\\ k_3(A)=A_j-A_{j'}+2n=0 & \forall m\in M,j,j'\in J,j'\ne j\\ k_4(A)=A_j-A_{j'}-n=0 & \forall m\in M,j,j'\in J,j'\ne j\\ k_5(x)=\sum\limits_{j=1}^{n}x_{j.o.m}-1\le 0 & \forall m\in M\\ k_6(t)=t_j^a-t_j^p\le 0 & \forall j\in J\\ k_7(m,n)=m-n\le 0 & \forall j\in J,\forall o\in O,\forall m\in M\\ k_8(A,P)=A_j-P_j\ge 0 & \forall j\in J \end{cases}$$

The Lagrangian objective function formed by handling the objective function and constraints of the OPSS stage is as follows.

Minimize total completion time:

$$\underset{t,x}{L}(t,x,\sum_{i=1}^{8}\lambda_i,\sum_{i=1}^{8}\varepsilon_i)=f_1(t,x)+\sum_{i=1}^{8}\sum_{i=1}^{8}\lambda_i k_i(t,x)+\sum_{i=1}^{8}\sum_{i=1}^{8}\varepsilon_i||k_i(t,x)||^2$$

Minimize total machine load:

$$\underset{A,P}{L}(A,P,\sum_{i=1}^{8}\lambda_i,\sum_{i=1}^{8}\varepsilon_i)=f_1(A,P)+\sum_{i=1}^{8}\sum_{i=1}^{8}\lambda_i k_i(A,P)+\sum_{i=1}^{8}\sum_{i=1}^{8}\varepsilon_i||k_i(A,P)||^2$$

Minimize maximum completion time:

$$\underset{t'}{L}(t',\sum_{i=1}^{8}\lambda_i,\sum_{i=1}^{8}\varepsilon_i)=f_1(t')+\sum_{i=1}^{8}\sum_{i=1}^{8}\lambda_i k_i(t')+\sum_{i=1}^{8}\sum_{i=1}^{8}\varepsilon_i||k_i(t')||^2$$

Similarly, the same method is used here to integrate the objective function, objective function vector, processed constraints, and other information into the improved fuzzy method for subsequent normalization and scaling of the objective function in the OPSS stage.

The Lagrangian objective function after processing the FFSS and OPSS is as follows:

Minimize total completion time for the entire process:

$$\underset{t,x}{L}(t,x,\sum_{i=1}^{8}\lambda_i,\sum_{i=1}^{8}\varepsilon_i,\sum_{i=1}^{10}\lambda_i,\sum_{i=1}^{10}\varepsilon_i)=L(t,x,\sum_{i=1}^{8}\lambda_i,\sum_{i=1}^{8}\varepsilon_i)+L(t,x,\sum_{i=1}^{10}\lambda_i,\sum_{i=1}^{10}\varepsilon_i)$$

Minimize machine total load for the entire process:

$$\underset{A,P,t,x}{L}(A,P,t,x,\sum_{i=1}^{8}\lambda_i,\sum_{i=1}^{8}\varepsilon_i,\sum_{i=1}^{10}\lambda_i,\sum_{i=1}^{10}\varepsilon_i) = L(A,P,\sum_{i=1}^{8}\lambda_i,\sum_{i=1}^{8}\varepsilon_i) + L(t,x,\sum_{i=1}^{10}\lambda_i,\sum_{i=1}^{10}\varepsilon_i)$$

Minimize maximum completion time for the entire process:

$$\underset{t'}{L}(t',\sum_{i=1}^{8}\lambda_i,\sum_{i=1}^{8}\varepsilon_i,\sum_{i=1}^{10}\lambda_i,\sum_{i=1}^{10}\varepsilon_i) = L(t',\sum_{i=1}^{10}\lambda_i,\sum_{i=1}^{10}\varepsilon_i) + L(t',\sum_{i=1}^{8}\lambda_i,\sum_{i=1}^{8}\varepsilon_i)$$

The objective function above represents the integration of the objective functions from both the OPSS stage and the FFSS stage, resulting in a complete production process objective function. This allows for the calculation of the distance between vectors under different objective functions.

4.2. Normalization and Same-Scale Transformation of the Objective Function

Since the constraints have been processed earlier, the Lagrangian objective functions L_1, L_2 and L_3 are normalized using normalization method. Let A and P represent the remaining thickness of the horizontal and longitudinal welds of the welding reel, respectively. These variables are only used as processing constraints and do not directly participate in time calculation. Therefore, they can be treated as constants in the Lagrangian objective function.

To map different objective functions to the [0, 1] interval, the following normalization function is set up:

$$h_i = \frac{L_i - L_{i,min}}{L_{i,max} - L_{i,min}}$$

i represents the number of objective functions, To normalize the integrated objective function L_1, L_2, L_3, we obtain:

$$\begin{cases} h_1(t,t',x) = \frac{L_1(t,x,\lambda,\varepsilon) - L_{1,min}(t,x,\lambda,\varepsilon)}{L_{1,max}(t,x,\lambda,\varepsilon) - L_{1,min}(t,x,\lambda,\varepsilon)} \\ h_2(t,t',x) = \frac{L_2(t,x,\lambda,\varepsilon) - f_{2,min}(t,x,\lambda,\varepsilon)}{f_{2,max}(t,x,\lambda,\varepsilon) - f_{2,min}(t,x,\lambda,\varepsilon)} \\ h_3(t,t',x) = \frac{L_3(t',\lambda,\varepsilon) - L_{3,min}(t',\lambda,\varepsilon)}{L_{3,max}(t',\lambda,\varepsilon) - L_{3,min}(t',\lambda,\varepsilon)} \end{cases}$$

Rearranging the above equation yields:

$$\begin{cases} h_1(t,t',x) = \frac{\sum_{j=1}^{n}\sum_{m=1}^{m}(t_j^x+t_j^y+t_j^z+t_j^a+t_j^b)x_{j,o,m} - \min(\sum_{j=1}^{n}\sum_{m=1}^{m}(t_j^x+t_j^y+t_j^z+t_j^a+t_j^b)x_{j,o,m})}{\max(\sum_{j=1}^{n}\sum_{m=1}^{m}(t_j^x+t_j^y+t_j^z+t_j^a+t_j^b)x_{j,o,m}) - \min(\sum_{j=1}^{n}\sum_{m=1}^{m}(t_j^x+t_j^y+t_j^z+t_j^a+t_j^b)x_{j,o,m})} \\ h_2(t,t',x) = \frac{\sum_{m=1}^{m}\sum_{o=1}^{k}\sum_{j=1}^{n}(t_{j,o,m}\cdot x_{j,o,m}) - min(\sum_{m=1}^{m}\sum_{o=1}^{k}\sum_{j=1}^{n}(t_{j,o,m}\cdot x_{j,o,m}))}{max(\sum_{m=1}^{m}\sum_{o=1}^{k}\sum_{j=1}^{n}(t_{j,o,m}\cdot x_{j,o,m})) - min(\sum_{m=1}^{m}\sum_{o=1}^{k}\sum_{j=1}^{n}(t_{j,o,m}\cdot x_{j,o,m}))} \\ h_3(t,t',x) = \frac{c_{j,o,m}(j\in J o\in O) - min(max_{j\in J}max_{o\in O}(c_{j,o,m}))}{max_{j\in J}max_{o\in O}(c_{j,o,m}) - min(max_{j\in J}max_{o\in O}(c_{j,o,m})} \end{cases}$$

The above formula solves the normalization problem for the three objective functions L_1, L_2, L_3 mentioned earlier. Meanwhile, To balance and compare objective functions with different measurement attributes on the same coordinate system, we process them as follows:

$$p_i(t,t',x) = \frac{1}{h_i(t,t',x) + \sum_{i=1}^{m}\frac{1}{h_i(t,t',x)} - m + 2}$$

After processing the normalized objective functions h_1, h_2, h_3 using the above equation, we obtain the same-scale objective functions as follows:

$$\begin{cases} p_1(t,t',x) = \frac{1}{h_1(t,t',x)+\frac{1}{h_1(t,t',x)}+\frac{1}{h_2(t,t',x)}+\frac{1}{h_3(t,t',x)}-1} \\ p_2(t,t',x) = \frac{1}{h_2(t,t',x)+\frac{1}{h_1(t,t',x)}+\frac{1}{h_2(t,t',x)}+\frac{1}{h_3(t,t',x)}-1} \\ p_3(t,t',x) = \frac{1}{h_3(t,t',x)+\frac{1}{h_1(t,t',x)}+\frac{1}{h_2(t,t',x)}+\frac{1}{h_3(t,t',x)}-1} \end{cases}$$

After normalization and standardization, the final objective functions p_1, p_2, and p_3 are obtained. These objective functions are used to calculate the distance between vectors and to filter dominated solutions and non-dominated solutions, ultimately yielding the optimal solution.

4.3. Processing of Objective Function Matrix

From the same-scale objective functions, we obtain the objective function vector $G = (p_1, p_2, p_3)$, which is used to generate the same-scale objective function matrix X, by substituting it into the following equation, where $x_{i,j}$ represents the value of the i-th variable under the j-th objective function:

$$\mathrm{X} = \begin{bmatrix} x_{11} & x_{12} & \cdots & x_{1j} \\ x_{21} & x_{22} & \cdots & x_{2j} \\ \vdots & \vdots & \ddots & \vdots \\ x_{i1} & x_{i2} & \cdots & x_{ij} \end{bmatrix}$$

Substituting the above matrix, we obtain the same-scale objective function vector matrix as follows:

$$\begin{bmatrix} p_{11} & p_{12} & p_{13} \\ p_{21} & p_{22} & p_{23} \\ p_{31} & p_{32} & p_{33} \end{bmatrix}$$
$$\Downarrow$$
$$\begin{bmatrix} \frac{1}{h_1(t)+\sum_{i=1}^{3}\frac{1}{h_i(t)}-2} & \frac{1}{h_2(t)+\sum_{i=1}^{3}\frac{1}{h_i(t)}-2} & \frac{1}{h_3(t)+\sum_{i=1}^{3}\frac{1}{h_i(t)}-2} \\ \frac{1}{h_1(t')+\sum_{i=1}^{3}\frac{1}{h_i(t')}-2} & \frac{1}{h_2(t')+\sum_{i=1}^{3}\frac{1}{h_i(t')}-2} & \frac{1}{h_3(t')+\sum_{i=1}^{3}\frac{1}{h_i(t')}-2} \\ \frac{1}{h_1(x)+\sum_{i=1}^{3}\frac{1}{h_i(x)}-2} & \frac{1}{h_2(x)+\sum_{i=1}^{3}\frac{1}{h_i(x)}-2} & \frac{1}{h_3(x)+\sum_{i=1}^{3}\frac{1}{h_i(x)}-2} \end{bmatrix}$$

Evaluating the distance between different objective function vectors using Euclidean distance:

$$\begin{cases} d_{t,t'} = \sqrt{(p_{11}(t)-p_{21}(t'))^2+(p_{12}(t)-p_{21}(t'))^2+(p_{13}(t)-p_{31}(t'))^2} \\ d_{t,x} = \sqrt{(p_{11}(t)-p_{31}(x))^2+(p_{12}(t)-p_{32}(x))^2+(p_{13}(t)-p_{33}(x))^2} \\ d_{x,t'} = \sqrt{(p_{31}(x)-p_{21}(t'))^2+(p_{32}(x)-p_{22}(t'))^2+(p_{33}(x)-p_{23}(t'))^2} \end{cases}$$

In the given equation, $d_{t,t'}$ represents the distance between vectors t, t' that represent the three objective functions. $d_{t,x}$ represents the distance between vectors t, x that represent the three objective functions. $d_{t',x}$ represents the distance between vectors t', x that represent the three objective functions. To determine whether a solution is non-dominated based on the calculated distance and subsequently filter it into the Pareto solution set.

4.4. Selection of Optimal Solution Based on TOPSIS

In the multi-objective optimization of steel pipe pile production scheduling, the same-scale objective function matrix X, Euclidean distance d, and adjusting parameter distance weight factor ω are used. The distance weight factor $w(j)$, between the solution vector and the existing solution vector in the Pareto front set PF is compared to determine whether the solution should be added to the set PF. Then, the simulated annealing algorithm is used to further search and optimize the solution set PF to improve the search effectiveness and result quality, and finally obtain a set of optimal Pareto solutions (see Figure 11). The solution set in the figure represents the optimal solution set under the condition of objective balance, which has been normalized and scaled and obtained through algorithmic filtering. A set of balanced optimization Pareto solution sets for total completion time, total machine load, and maximum completion time are obtained (see Algorithms 1 and 2 for details).

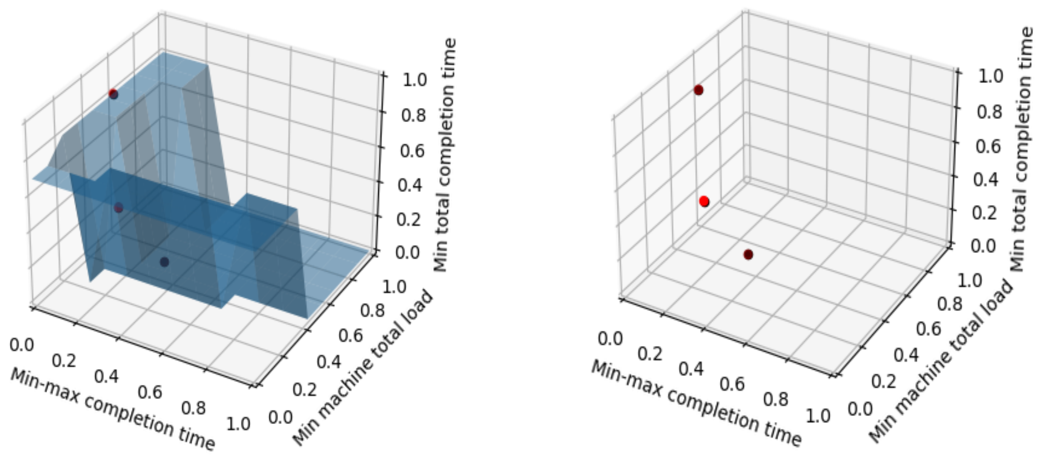

Figure 11. Pareto Optimal Solution.

The TOPSIS method is an effective way to comprehensively evaluate different Pareto front solutions. By obtaining the positive and negative ideal solutions and combining them with the weight vector, we can calculate the distance between each solution in the front set and the positive/negative ideal solutions. Then, by calculating the relative closeness of each solution and sorting them, we can obtain the optimal solution.

Based on the actual production situation of OWTSPP, enterprise decision-makers assign weights to three objective functions: total completion time, maximum completion time, and machine utilization rate, represented as ω = (0.5, 0.3, 0.2). The weighted standardized matrix V is calculated as follows:

$$v_{ij} = w_j \times x_{ij}$$

The positive and negative ideal solutions are then calculated as follows:

$$x_j^+ = max(v_{ij}),\ x_j^- = min(v_{ij})$$

Calculate the distance between each solution vector and the positive/negative ideal solutions:

$$s_i^+ = \sum_{j=1}^{m} |v_{ij} - x_j^+|$$

$$s_i^- = \sum_{j=1}^{m} |v_{ij} - x_j^-|$$

The relative closeness of each solution vector is then calculated as follows:

$$C_i = \frac{s_i^-}{s_i^+ + s_i^-}$$

We obtain the positive ideal solution $x^+ = (0.144, 0.31, 0.225)$, and negative ideal solution $x^- = (0, 0, 0)$. Sorting all solution vectors according to their relative closeness C_i, we select the top-ranked solution vector as the optimal solution, see Table 6.

Table 6. Ranking of Evaluation Solutions Using TOPSIS.

Serial Number	s_i^+	s_i^-	C_i	Ranking
1	0.144	0.535	0.787	1
2	0.349	0.33	0.486	2
3	0.463	0.216	0.318	3

4.5. Optimal vs. Empirical Scheduling: A Comparative Analysis

A certain heavy industry enterprise schedules the production of OWTSPP in the workshop based on expert experience. The effect of the experience schedule is shown in Figure 12, and the production completion time is about 56 h. Managers allocate personnel to operate machines based on experience, with fixed personnel operating designated machines to process designated processes. In case of urgent production needs, temporary personnel may be recruited or transferred for production (mathematical symbols and interpretation are shown in Part (a) of Nomenclature Section).

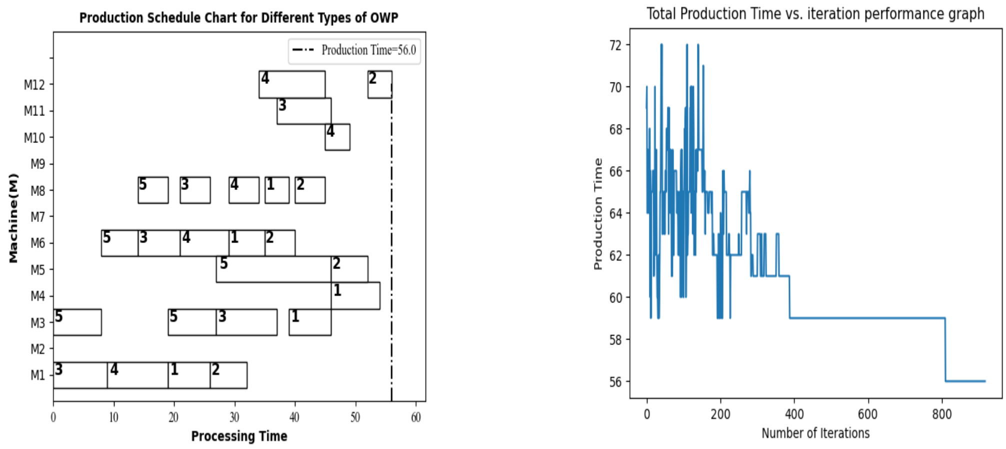

Empirical Scheduling Plan for Five OWTSPP Production

Empirical Scheduling Plan Time Consumption

Figure 12. Results of the Empirical Scheduling Plan.

By using the TOPSIS method to rank the Pareto optimal solutions obtained from multi-objective optimization, it was found that Solution 1 had the highest score of 0.787 and was identified as the best solution. Figure 13 displays the scheduling plan where the production completion time is 48 h under the optimal schedule, which is 8 h shorter compared to the production time under the empirical scheduling approach. This results in a 14.29% increase in production efficiency. The comparison of the total production time between the empirical scheduling approach and the optimal solutions for the 5 steel pipe pile scheduling is shown in Figure 14. The blue line represents the possible shortest total completion time under the empirical scheduling approach, while the orange line represents the possible shortest total completion time under the optimal scheduling condition.

In order to verify the practicality of the method in large-scale scheduling, the production quantity of each type of steel pipe pile was increased to 5, totaling 25 OWTSPP. The production situation under empirical scheduling and optimal scheduling was compared (see Figures 15 and 16). It can be seen in Figure 17 that under the empirical scheduling approach, the production completion time for the 25 OWTSPP was 201 h, while under the optimal scheduling plan, the production completion time was reduced to 166 h, resulting in a reduction of 35 h and an increase in production efficiency by 17.41%. This shows that the method has more advantages in solving large-scale production problems.

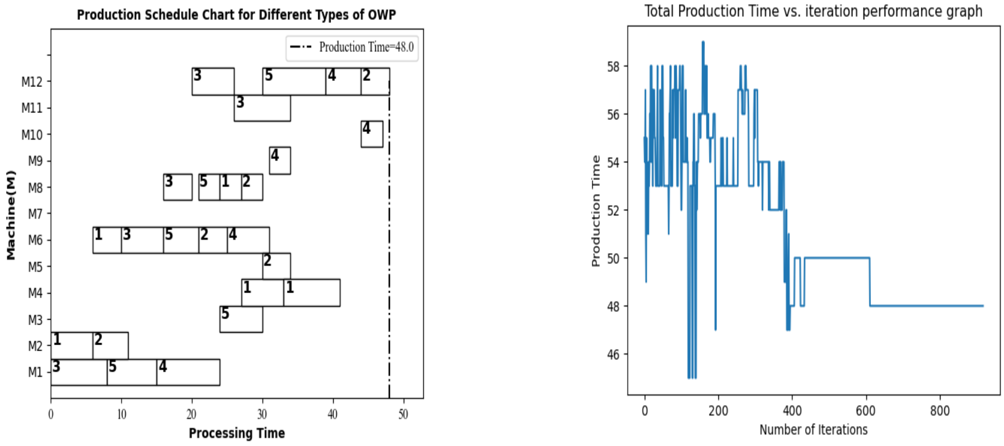

Optimal Scheduling Plan for Five OWTSPP Production

Optimal scheduling Plan Time Consumption

Figure 13. Results of the Optimal Scheduling Plan.

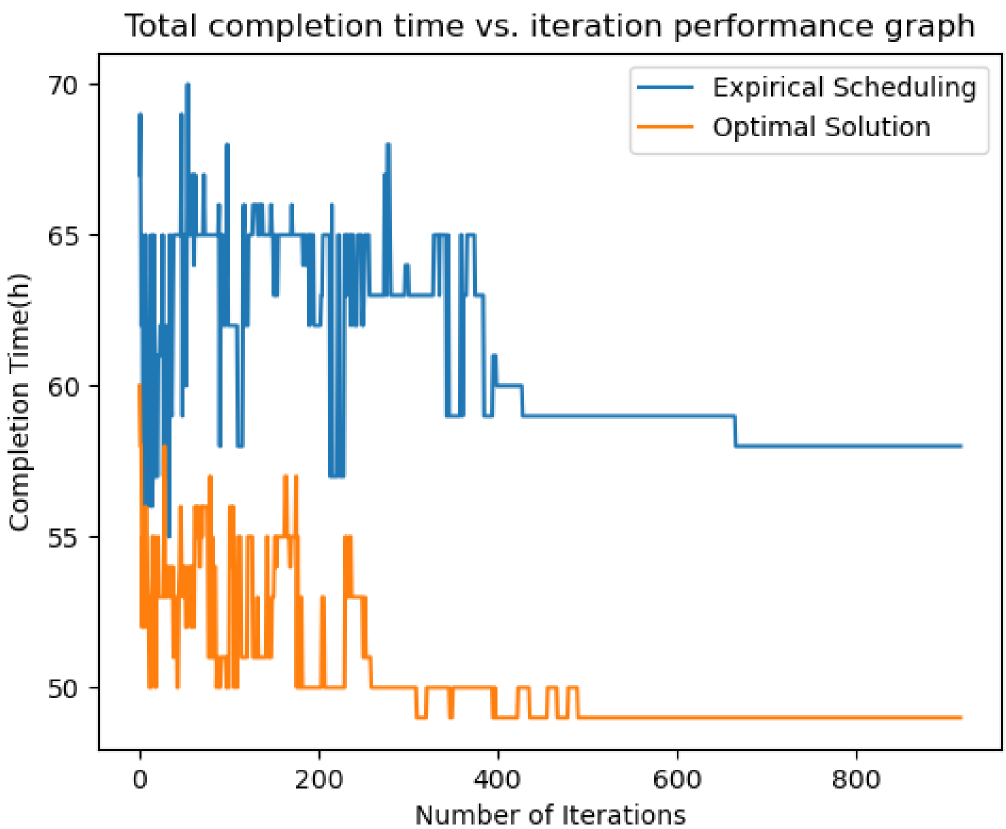

Figure 14. Comparison of Production Time: Empirical vs. Optimal.

The comparison of the production completion time between the empirical scheduling approach and the optimal solution obtained from the improved method for large-scale scheduling is shown in Figure 18. The blue line in the figure represents the possible shortest total completion time under the empirical scheduling approach; The orange line represents the possible shortest total completion time under the optimal scheduling condition.

Therefore, in practical manufacturing, this method can effectively improve production efficiency, reduce production costs, and bring more economic benefits to enterprises. The data content is shown in Tables 3–5. The algorithm for extracting data and generating a scheduling Gantt chart can be found in Appendix A.

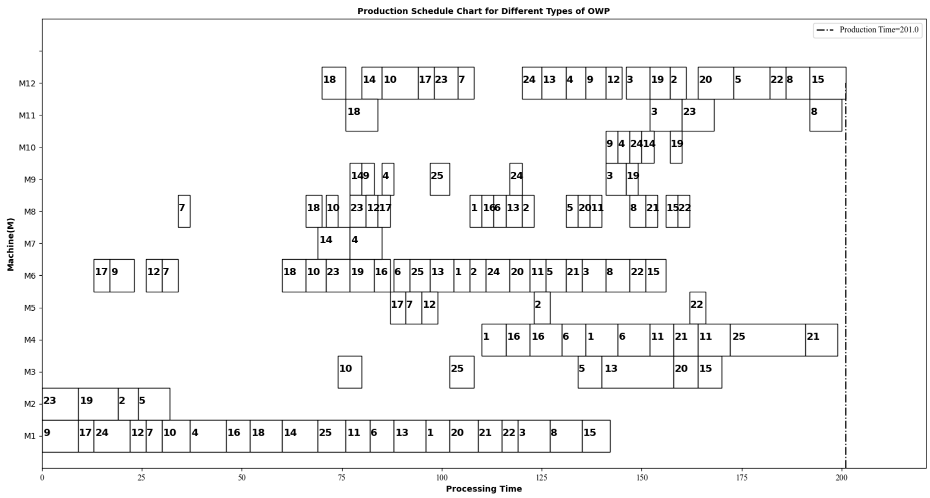

Figure 15. Mass Production: Empirical Scheduling Scheme.

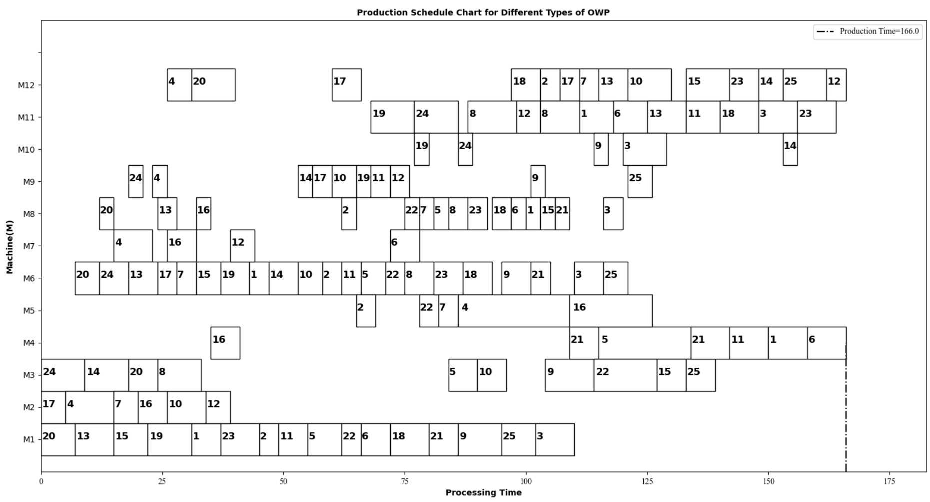

Figure 16. Mass Production: Optimal Scheduling Scheme.

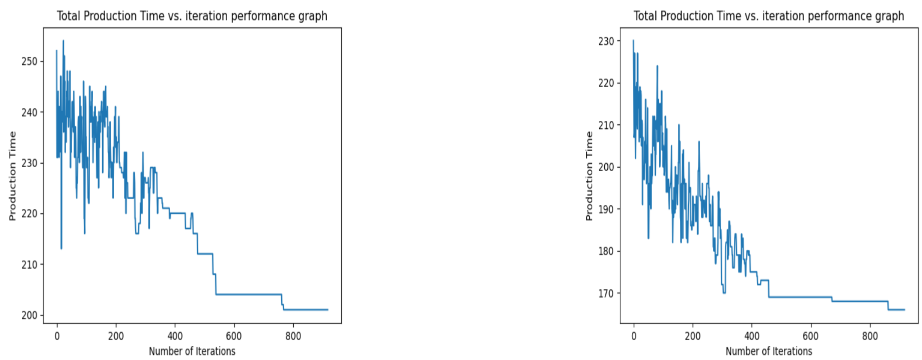

Empirical Scheduling Plan Time Consumption

Optimal Scheduling Plan Time Consumption

Figure 17. Production Time for Empirical Scheduling and Optimal Scheduling in Large-scale Production.

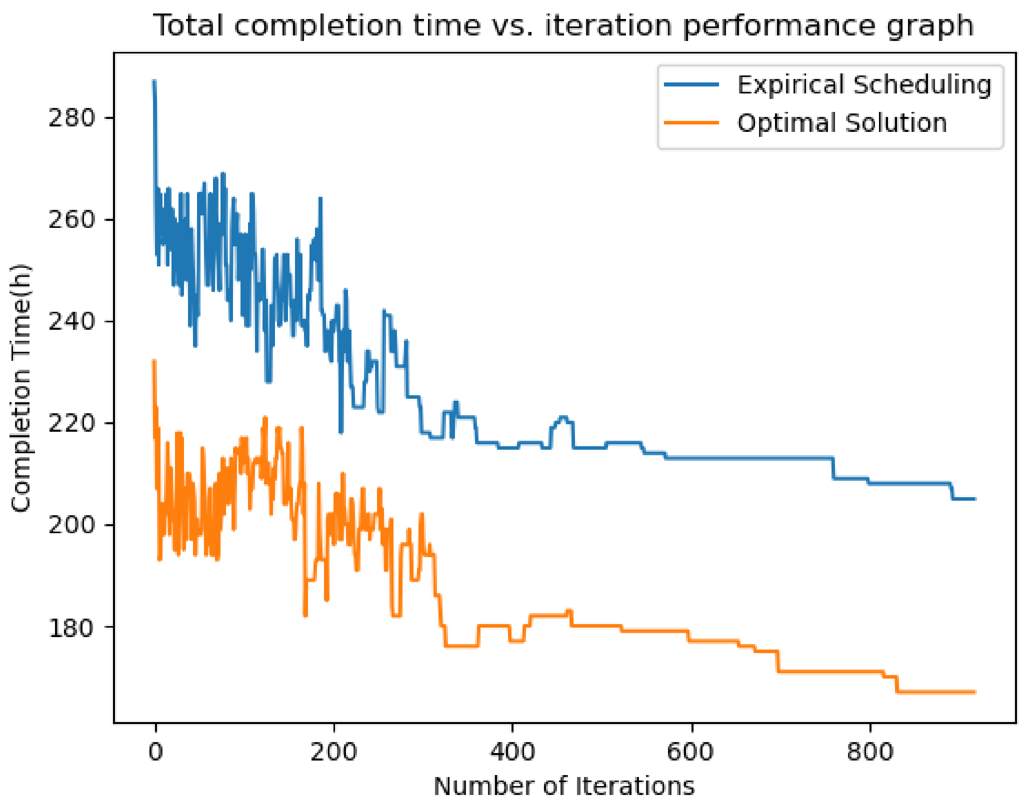

Figure 18. Empirical vs. Optimal: Total Production Time in Large-Scale Scheduling.

5. Disscussion

In this section, we discuss the advantages and disadvantages of the proposed method. Firstly, we divide the entire production process into two stages, FFSS and OPSS, according to the characteristics of different production Stages. In each stage, we optimize the scheduling process and objective functions separately, which simplifies the problem handling. We also consider the slack time and incorporate it into the production processes along with the disjunctive graph model, greatly facilitating the modeling of the production processes. Secondly, for the constraints and objective functions, we use the extended Lagrange multiplier method with penalty terms to handle them effectively. Lastly, we introduce the hesitant fuzzy approach, extending it to a multi-dimensional method that includes vectors, objective functions, and constraints, This makes the handling of constraints and objective functions more convenient. Moreover, this method is not affected by the initial weights of the objective functions during the screening of Pareto front solutions. Instead, the weighted values are assigned to the filtered Pareto solutions, enabling better selection of the optimal solution. We do not provide initial weights for the objective functions, ensuring the normalization and scaling conditions during the objective function processing. As a result, we obtain a set of well-filtered Pareto front solutions.

However, this method also has some issues in terms of solution filtering. For example, some potential solutions may be eliminated through the screening process, leading to a set of solutions that appear to be a Pareto front, but in reality, some solutions may have been lost during the filtering process.

6. Conclusions and Future Works

In this paper, we analyze the multi-objective scheduling optimization problem in steel pipe pile production and propose an improved hesitant fuzzy method. We extend the dimensions in the model to include objective functions, objective function vectors, and constraints, considering all relevant important condition parameters. To handle multiple constraints and multiple objective functions, we utilize the Lagrange multiplier method with penalty terms to process the multiple constraints and generate the Lagrangian objective function. Additionally, we map the actual production process onto a disjunctive graph model, providing a clear visualization of the production timeline. By combining the Pareto front algorithm with the simulated annealing algorithm, we filter and obtain the Pareto front solution set and rank the obtained solutions using the TOPSIS method. Ultimately, we derive the optimal solution along with its corresponding scheduling plan.

Compared to previous multi-objective scheduling optimization methods, the approach proposed in this paper introduces a novel way of handling objective functions and constraints. By utilizing hesitant fuzzy method and calculating the normalized and scaled Euclidean distance of objective function vectors, this method can more accurately eliminate dominated solutions and improve the quality of Pareto front solutions.

This paper demonstrates that under the production data of 5 different types of OWT-SPP, the optimal solution obtained using the improved method proposed in this paper reduces the production time by about 8 h and improves the production efficiency by approximately 14.29% compared to the empirical scheduling approach. In large-scale production, the production time is reduced by approximately 35 h, and the production efficiency is increased by about 17.41%.

The proposed method in this paper provides a reference for integrating the objective function and its constraints to find Pareto non-dominant solutions and serves as a screening tool during the process. However, due to space limitations, the superiority of the proposed method over various multi-objective algorithms in terms of evaluation indicators has not been verified as a completely new algorithm. The reliability of the method under more than three objective functions has not been tested in the steel pipe pile scheduling example. Further research is needed to test the reliability of this method when it includes more solution vectors for multi-objective optimization. These aspects will be the focus of future research. It is hoped that this paper can promote the development and application of the proposed method in industrial production through academic research.

Author Contributions: Conceptualization, W.W. and J.X.; methodology, W.W.; algorithm, W.W.; software support, W.W. and S.W.; validation, W.W. and Z.W.; logic and principle analysis, J.X.; investigation, W.W. and S.W.; resources, D.F. and J.X.; data curation, W.W. and S.W.; writing—original draft preparation, W.W. and D.F.; writing—review, Z.W. and D.F.; diagram design, W.W. and Z.W.; supervision, D.F. and J.X.; project administration, J.X. and D.F.; funding acquisition, J.X. All authors have read and agreed to the published version of the manuscript.

Funding: This research is supported by the National Key Research and Development Program (Grant No. 2021YFB3301805) and the Nansha District Science and Technology Project, Guangzhou, Guangdong Province, China (Grant No. 2021ZD008).

Institutional Review Board Statement: Not applicable.

Informed Consent Statement: Not applicable.

Data Availability Statement: Not applicable.

Conflicts of Interest: The authors declare no conflict of interest. The funders had no role in the design of the study; in the collection, analyses, or interpretation of data; in the writing of the manuscript, or in the decision to publish the results.

Nomenclature

(a) Mathematical Symbols and Interpretation

Symbols	Explanation
J	Job set, $J = j_1, j_2, \ldots, j_n$
M	Machine set, $M = m_1, m_2, \ldots, m_m$
M_{ai}	Welder Set, $M_a = m_1, m_2, m_3, m_4, m_5, m_{10}, m_{11}, m_{12}$
M_{bi}	Cutter Set, $M_b = m_6, m_7$
M_{ci}	Rolling Mill Set, $M_c = m_8, m_9$
O	Process set, $O = o_1, o_2, \ldots, o_o$
$b_{j,m,t}$	The load of machine m at time t
$x_{j,o,m}$	Whether welding machine j is idle or not, with a value of 1 indicating that the machine has a welding task and a value of 0 indicating no task.
E_j	The maximum allowable lead time indicator for workpiece j which represents the expected completion time.
D_j	The delivery time of workpiece j.
C_j	The total completion time of workpiece j.
$s_{j,o,m}$	The start time of operation o of workpiece j on machine m.
$c_{j,o,m}$	The completion time of operation o of workpiece on machine m.
$t_{j,o,m}$	The processing time of the oth operation of workpiece j on machine m.
t_j^x	The time required for workpiece j during the steel plate splicing operation.
t_j^y	The time required for workpiece j during the steel plate cutting operation.
t_j^z	The time required for workpiece j during the steel plate rolling operation.
t_j^a	The time required for longitudinal welding of workpiece$j$.
t_j^b	The time required for circumferential welding of workpiece j.
t_j	The total processing time of workpiece j in all operations.
t_{c1}	The time required for the first intermediate transfer.
t_{c2}	The time required for the second intermediate transfer.
t_{c3}	The time required for the third intermediate transfer.
t_{c4}	The time required for the forth intermediate transfer.
t_c	The total time required for intermediate transfers.
n	Number of jobs
m	Number of machines
j,j'	Different workpiece numbers.
m,m'	Different machine numbers.

(b) Symbol and Interpretation Information Table

Acronym	Definition
SPS	Steel plate splicing
SPC	Steel plate cutting
RP	Rolling pipe
LW	Longitudinal welding
CW	Circumferential welding
B.Crane	Bridge crane
C.Crane	Cantilever crane
O.Crane	Overhead crane
WCM	Wire consumption per meter
MPC	Monthly production capacity
WS	Workstation
WH	Processing time for each step
OUT	Output
M/W Qty	Machine/Workstation quantity
SW Pro. E	Single workstation production efficiency
W.H	Working hours
OWTSPP-PF	OWTSPP processing frequency

Appendix A. Here Is the Algorithm for Extracting Data and Drawing a Scheduling Gantt Chart

Algorithm A1 Scheduling Gantt Chart Generation Algorithm

```
FUNCTION Scheduling(n, m, pi, data)
    $s_{jom}$, $t_{jom}$, tdx, $O$, tom = data[1], data[2], data[3], data[4], data[5]
    FUNCTION create-job()
    job $< -$ RANDOMLY PERMUTE $O$ INTO A 1D ARRAY AND
    RESHAPE TO SHAPE (1, length of $O$)
    $M$ <- RANDOMLY SELECT VALUES FROM $s_{jom}$ ACCORDING TO job
    $t_{jom}$ <- RANDOMLY SELECT VALUES FROM $t_{jom}$ ACCORDING TO job
    RETURN job, $M$, $t_{jom}$
FUNCTION calculate(job, $M$, $t_{jom}$)
    tmm <- ZERO MATRIX OF SHAPE (1, $m$)
    $list_M$, $list_S$, $list_W$ <- EMPTY LISTS
    FOR $i$ IN range(length of job) DO
        svg <- job[$i$]
        sig <- $M$[$i$] - 1
        startime <- MAXIMUM VALUE IN tmm[0, sig]
        tmm[0, sig] <- startime + $t_{jom}$[i]
        ADD $M$[$i$] TO $list_M$
        ADD startime TO $list_S$
        ADD $t_{jom}$[$i$] TO $list_W$
    $c_{jom}$ <- MAXIMUM VALUE IN tmm[0]
    RETURN $c_{jom}$, $list_M$, $list_S$, $list_W$
FUNCTION draw(job, $M$, $t_{jom}$)
    $c_{jom}$, $list_M$, $list_S$, $list_W$ <- calculate(job, $M$, $t_{jom}$)
    RETURN None
```

Algorithm A2 Data Extraction Algorithm

```
DataDeal(self, $n$, $m$):
    self.$n$= $n$
    self.$m$ = $m$
def read-data(self):
    data = np.loaddata('./data', skiprows=1)
    return data
def calculate-schedule(self):
    data = self.read-data()
    $s_{jom}$ = np.zeros((self.$n$, self.$m$))
    $t_{jom}$ = np.zeros((self.$n$, self.$m$))
    $O$ = []
    tdx = []
    tom = []
    for $i$ in range(self.$n$):
        $M$, $t_{jom}$ = data[$i$][1::2], data[$i$][2::2]
        $s_{jom}$[$i$][:len($M$)] = $M$
        tmm[0, sig] <- startime + $t_{jom}$[$i$]
        $t_{jom}$[$i$][:len($t_{jom}$)] = $t_{jom}$
        $O$.extend([$i$] * len($M$))
        curr-tdx = []
    **for** $j$ in range(len($M$))
            curr-tdx.append(sum($s_{jom}$[$i$][0:j + 1]))
        tdx[$-1$] = curr-tdx
        tom.append(curr-tdx)
    **return** $s_{jom}$, $t_{jom}$, $O$, tdx, tom
```

References

1. Johnson, S.M. Optimal two-and three-stage production schedules with setup times included. *Nav. Res. Logist. Q.* **1954**, *1*, 61–68. [CrossRef]
2. Chaudhry, I.A.; Khan, A.A. A research survey: Review of flexible job shop scheduling techniques. *Int. Trans. Oper. Res.* **2016**, *23*, 551–591. [CrossRef]
3. Xie, J.; Gao, L.; Peng, K.; Li, X.; Li, H. Review on flexible job shop scheduling. *IET Collab. Intell. Manuf.* **2019**, *1*, 67–77. [CrossRef]
4. Guohui, Z. Research on Methods for Flexible Job Shop Scheduling Problems. Ph.D. Thesis, Huazhong University of Science and Technology, Wuhan, China, 2009.
5. Binhuang, Y. Review on flexible flow shop scheduling. *Mod. Manuf. Eng.* **2022**, *9*, 154–162. [CrossRef]
6. Zeng, Q.; Yang, Y.; Wang, X.L.; Wen, Y. Multi-objective optimization method for equal lot scheduling problem of Job Shop with parallel machines. *Comput. Integr. Manuf. Syst.* **2011**, *4*, 816–825. [CrossRef]
7. Xie, G.; Pan, Y.; Li, J. Multi-objective optimization algorithm for hybrid flow shop scheduling problem. *Comput. Eng. Des.* **2018**, *39*, 885–889.
8. Lawler, E.L. Optimal sequencing of a single machine subject to precedence constraints. *Manag. Sci.* **1973**, *19*, 544–546. [CrossRef]
9. Shen, C.; Chen, Y.; Chou, F.D.; Huang, P. Bi-objective Optimization for Scheduling on Identical Parallel Machine Considering Preventive Maintenance and Job's Release Time. In Proceedings of the 2021 3rd International Conference on Machine Learning, Big Data and Business Intelligence (MLBDBI), Taiyuan, China, 3–5 December 2021; pp. 630–637.
10. Yeh, W.C.; Chuang, M.C.; Lee, W.C. Uniform parallel machine scheduling with resource consumption constraint. *Appl. Math. Model.* **2015**, *39*, 2131–2138. [CrossRef]
11. Kaabi, J.; Harrath, Y. A survey of parallel machine scheduling under availability constraints. *Int. J. Comput. Inf. Technol.* **2014**, *3*, 238–245.
12. Wang, Y.; Feng, Y.; Gao, Y.C. Multi-objective optimization method of flexible job-shop lot-splitting scheduling. *J. Zhejiang Univ.* **2011**, *4*, 719–726.
13. Dong, H.; Xu, X.; Xie, X. Solving Multi-flexible Job-shop Scheduling by Multi-objective Algorithm. *Comput. Sci.* **2020**, *12*, 239–244.
14. Liefooghe, A.; Basseur, M.; Jourdan, L.; Talbi, E.G. Combinatorial optimization of stochastic multi-objective problems: An application to the flow-shop scheduling problem. In Proceedings of the Evolutionary Multi-Criterion Optimization: 4th International Conference, EMO 2007, Matsushima, Japan, 5–8 March 2007; Proceedings 4, pp. 457–471.
15. Talbi, E.G.; Basseur, M.; Nebro, A.J.; Alba, E. Multi-objective optimization using metaheuristics: Non-standard algorithms. *Int. Trans. Oper. Res.* **2012**, *19*, 283–305. [CrossRef]
16. Cheng, Q.; Gao, Y.; Chu, H.; Zhang, C.; Liu, Z. Flexible Job Shop Scheduling of Machining Based on Multi- objective Differential Evolution Algorithm. *J. Beijing Univ. Technol.* **2023**, *3*, 335–345.
17. Li, C.; Li, T.; Wang, Z.; Gu, P.E.; Lin, D. An improved genetic algorithm based on multi-objective optimization is used to solve the flexible job-shop scheduling problem. *Manuf. Technol. Mach. Tool* **2023**, *5*, 173–178. [CrossRef]
18. Wang, T.; Liu, D. Multi-objective Optimization Method for Automated Dismantling Production Line of Retired Automobiles under Rigid Constraints. *Mach. Build. Autom.* **2023**, *52*, 184–188. [CrossRef]
19. Zhu, X. Flexible Job Shop Scheduling Multi-object Optimization Based on Strong Reproduction NSGA-II Algorithm. *Modul. Mach. Tool Autom. Manuf. Tech.* **2021**, *9*, 180–184. [CrossRef]
20. Zhang, G.; Gao, L.; Shi, Y. An effective genetic algorithm for the flexible job-shop scheduling problem. *Expert Syst. Appl.* **2011**, *38*, 3563–3573. [CrossRef]
21. Fanjul-Peyro, L.; Perea, F.; Ruiz, R. Models and matheuristics for the unrelated parallel machine scheduling problem with additional resources. *Eur. J. Oper. Res.* **2017**, *260*, 482–493. [CrossRef]
22. Yamashiro, H.; Nonaka, H. Estimation of processing time using machine learning and real factory data for optimization of parallel machine scheduling problem. *Oper. Res. Perspect.* **2021**, *8*, 100196. [CrossRef]
23. Goh, C.K.; Tan, K.C. Evolutionary multi-objective optimization in uncertain environments. *Issues Algorithms Stud. Comput. Intell.* **2009**, *186*, 5–18.
24. Le, Z. Study on Multi-Objective Dynamic Production Scheduling Problem of Flexible Job-Shop under Uncertainty. Master's Thesis, Beijing Jiaotong University, Beijing, China, 2015.
25. Zhong, X.; Han, Y.; Yao, X.; Gong, D.; Sun, Y. An evolutionary algorithm for the multi-objective flexible job shop scheduling problem with uncertain processing time. *Sci. Sin.* **2023**, *4*, 737–757. [CrossRef]
26. Yogashanthi, T.; Sathish, S.; Ganesan, K. Generalized Intuitionistic Fuzzy Flow Shop Scheduling Problem with Setup Time and Single Transport Facility. *Int. J. Fuzzy Log. Intell. Syst.* **2023**, *23*, 34–43. [CrossRef]
27. Srivastava, G.; Singh, A. An evolutionary approach comprising tailor-made variation operators for rescue unit allocation and scheduling with fuzzy processing times. *Eng. Appl. Artif. Intell.* **2023**, *123*, 106246. [CrossRef]
28. Ishibuchi, H.; Yamamoto, N.; Misaki, S.; Tanaka, H. Local search algorithms for flow shop scheduling with fuzzy due-dates. *Int. J. Prod. Econ.* **1994**, *33*, 53–66. [CrossRef]
29. Ishii, H.; Tada, M.; Masuda, T. Two scheduling problems with fuzzy due-dates. *Fuzzy Sets Syst.* **1992**, *46*, 339–347. [CrossRef]
30. Xie, Y.; Xie, J.; Deng, X. Fuzzy Single Machine Scheduling Problem with Mixed Precedence Constraints and Fuzzy Due Dates. *Inf. Control* **2005**, *34*, 369–372.
31. Litoiu, M.; Tadei, R. Real time task scheduling allowing fuzzy due dates. *Eur. J. Oper. Res.* **1997**, *100*, 475–481. [CrossRef]

32. Chanas, S.; Kasperski, A. On two single machine scheduling problems with fuzzy processing times and fuzzy due dates. *Eur. J. Oper. Res.* **2003**, *147*, 281–296. [CrossRef]
33. Khalifa, H.A.E.W.; Smarandache, F.; Alodhaibi, S.S. A fuzzy approach for minimizing machine rental cost for a specially-structured three-stages flow-shop scheduling problem in a fuzzy environment. In *Handbook of Research on Advances and Applications of Fuzzy Sets and Logic*; IGI Global: Hershey, PA, USA, 2022; pp. 105–119.
34. Sun, M.; Cai, Z.; Zhang, H. A teaching-learning-based optimization with feedback for LR fuzzy flexible assembly job shop scheduling problem with batch splitting. *Expert Syst. Appl.* **2023**, *224*, 120043. [CrossRef]
35. Wang, H.J.; Zhu, G.Y. Multiobjective Optimization for FJSP under Immediate Predecessor Constraints Based OFA and Pythagorean Fuzzy Set. *IEEE Trans. Fuzzy Syst.* 2023, *early access*. [CrossRef]
36. Hu, C.F.; Teng, C.J.; Li, S.Y. A fuzzy goal programming approach to multi-objective optimization problem with priorities. *Eur. J. Oper. Res.* **2007**, *176*, 1319–1333. [CrossRef]
37. Li, X.; Wang, D.; Li, K.; Gao, Z. A green train scheduling model and fuzzy multi-objective optimization algorithm. *Appl. Math. Model.* **2013**, *37*, 2063–2073. [CrossRef]
38. Gholamian, N.; Mahdavi, I.; Tavakkoli-Moghaddam, R. Multi-objective multi-product multi-site aggregate production planning in a supply chain under uncertainty: Fuzzy multi-objective optimisation. *Int. J. Comput. Integr. Manuf.* **2016**, *29*, 149–165. [CrossRef]
39. Li, S. Pythagorean Fuzzy Multi-Attribute Group Decision Making Method and Its Application. Master's Thesis, Jiangxi University of Finance and Economics, Nanchang, China, 2019.
40. Zhen, J. Research on Multi-Criteria Group Decision Making Theories and Methods with Pythagorean Fuzzy Sets. Ph.D. Thesis, Jiangxi University of Finance and Economics, Nanchang, China, 2019.
41. Zhang, X.; Xu, Z. Extension of TOPSIS to multiple criteria decision making with Pythagorean fuzzy sets. *Int. J. Intell. Syst.* **2014**, *29*, 1061–1078. [CrossRef]
42. Liu, W.; He, X. Pythagorean Hesitant Fuzzy Set. *Fuzzy Syst. Math.* **2016**, *30*, 107–115.
43. Liu, W.; He, X.; Chang, J. Correlation measures of Pythagorean hesitant fuzzy set. *Control Decis.* **2019**, *34*, 1018–1024. [CrossRef]
44. He, X.; Liu, W.; Du, Y. Pythagorean hesitant fuzzy aggregation operators and their applications in decision making. *Appl. Res. Comput.* **2020**, *37*, 2338–2343. [CrossRef]
45. Du, X.; Li, Y.; Li, Q.; Qin, S. Exactness Properties of the Hestenes-Powell Augmented Lagrangian Function for Inequality Constrained Optimization Problems. *Chin. J. Eng. Math.* **2009**, *1*, 138–146.
46. Liang, C. Some Augmented Lagrangian Function Based Methods for Constrained Optimization. Ph.D. Thesis, Hunan University, Changsha, China, 2016.
47. Yu, X.; Xu, Z.; Chen, Z.; Xu, Z. Lagrange Neural Network for Nonsmooth Nonconvex Optimization Problems with Equality and Inequality Constrains. *J. Electron. Inf. Technol.* **2017**, *39*, 1950–1955.
48. Du, X. Augmented Lagrangian Function Methods for Solving Constrained Optimization Problems. Ph.D. Thesis, Shanghai University, Shanghai, China, 2005.
49. Du, X.; Jin, Z. An Exact Augmented Lagrangian Function for Nonlinear Programming Problems with Inequality Constraints. *J. Shanghai Jiaotong Univ.* **2006**, *9*, 1636–1640. [CrossRef]